EXPERIMENTAL DETERMINATION OF MATERIAL PARAMETERS USING STABILIZED CYCLE TESTS TO PREDICT THERMAL RATCHETTING

Mohammad ZEHSAZ[1], Farid Vakili TAHAMI [2] and Hassan AKHANI[3]

In this paper to predict the ratchetting, kinematic hardening parameters C, γ, isotropic hardening parameters and also k, b, Q combined isotropic/kinematic hardening parameters have been obtained experimentally , from the monotonic, Strain controlled condition and cyclic tests at room(20 ^{o}c) and elevated temperatures 350 ^{o}c and 600 ^{o}c . These parameters are used in nonlinear combined isotropic/kinematic hardening model to predict better description of loading and reloading cycles in cyclic indentation as well as thermal ratcheting. For this purpose three group specimens of Stainless steel 304L and Carbon Steel investigated. After each test and using stable hysteresis cycles material parameters have been obtained for using in combined nonlinear isotropic/kinematic hardening models. Also the methodology of obtaining the correct kinematic/isotropic hardening parameters is presented in the article.

Keywords: Thermal ratcheting, Cyclic loading, Stabilized Cycle tests, Combine hardening parameters

1. Introduction

The literature review shows that accurate closed form solutions may not be found to analyses the ratchetting behavior of the pressurized vessels under cyclic thermal loading. However, approximate solutions have been developed by Wada et al. (1993), Wada et al. (1989), Uga (1974), Bree (1967), Edmunds (1961) and Miller(1959) which can be used to calculated the induced incremental plastic strains caused by ratchetting.

The evaluation procedures of thermal ratchetting in the present thermal ratchetting design ASME rules show that the primary stresses play an important role so that they do not cover the case of ratchetting under pure or dominant thermal cyclic loads. However, the ratchetting deformation can occur under the null-primary-stress condition by Igari T (1993). Hyeong-Yeon Lee (2002) investigated thermal ratchetting deformation of a 316L stainless steel cylindrical structure under an axial moving temperature distribution.

[1] Prof., Dept.of Mech. Eng., University of Tabriz, Iran, e-mail:zehsaz@tabrizu.ac.ir
[2] Associate Prof., Dept.of Mech. Eng., University of Tabriz, Iran, e-mail: f_vakili@tabrizu.ac.ir
[3] M.Sc., Dept.of Mech. Eng., University of Tabriz, Iran, e-mail: h_akhani89@ms.tabrizu.ac.ir

The ratchetting occurs under the prescribed asymmetrical cyclic stressing for materials, and ratchetting strain increases progressively cycle by cycle. However, the materials do display some differences in ratchetting behavior. When the nonlinear isotropic/kinematic hardening model is used, the center of the yield surface moves in stress space due to the kinematic hardening component and the yield surface range may expand due to the isotropic due to the isotropic component. These features allow modeling of inelastic deformation in metals that are subjected to cycles of load or temperature, resulting in significant inelastic deformation and, possibly, low cycle fatigue failure. The nonlinear isotropic/kinematic hardening model can provide more accurate results in many cases involving cyclic loading. Typically, transient ratchetting is followed by stabilization (zero ratchet strain) for low mean stresses, while constant increase in the accumulated ratchet strain is observed at high mean stresses. The nonlinear kinematic hardening component, used without the isotropic hardening component, predicts constant ratchet strain Combined hardening properties of nonlinear isotropic/kinematic hardening model to predict the cyclic loading behavior of the structures. In this study, stress–strain data and material parameters have been obtained from several stabilized cycles of specimens that are subjected to symmetric strain cycles (Zakavi et al). Use of this model requires the hardening parameters. In this work Material parameters are determined experimentally using monotonic and stabilized Cycles at room and elevated 350^0c and 600^0c for used Combined hardening model that this Models is more accurate results to predict progressive loading condition Course gives strains.

2. Hardening model

The isotropic and kinematic hardening models are used to simulate the inelastic behavior of materials that are subjected to cyclic loading. The use of plasticity material models with isotropic type hardening is generally not recommended since they continue to harden during cyclic loading. The isotropic hardening model always predicts shakedown behavior, if creep is not considered . The kinematic hardening plasticity models are proposed to model the inelastic behavior of materials that are subjected to repeated loading. For example, the Armstrong–Frederick kinematic hardening model (1966) is suggested for the nonlinear strain hardening materials. Based on the Armstrong–Frederick nonlinear kinematic hardening rule, many constitutive models have been constructed to simulate the uniaxial and multiaxial ratchetting of materials characterized by cyclic hardening or cyclic stable behaviors. The results of these models are discussed for structures under various types of cyclic loads in references (Rahman et al., 2008; Mahbadi and Eslami, 2006; Eslami and Mahbadi, 2001; Prager, 1956). kinematic hardening model or a (combined) nonlinear isotropic/kinematic hardening model may be used to simulate the behavior of materials that are

subjected to cyclic loading. The evolution law in these models consists of a kinematic hardening component which describes the translation of the yield surface in the stress space. An isotropic component which describes the change of the elastic range is added for the nonlinear isotropic/kinematic hardening model.

2.1. Isotropic hardening model

The isotropic hardening model which describes the change of the elastic range is discussed here. The isotropic hardening means that the yield surface changes size uniformly in all directions such that yield stress increases in all stress directions as plastic straining occurs.

According to the isotropic hardening rule, the evolution of the loading surface is governed only by one scalar variable, R. For time independent plasticity and isothermal plastic deformation, the yield surface is expressed as (Lemaitre and Chaboche, 1994):

$$f = f(\sigma, R) \tag{1}$$

The above equation, considering the von-Mises criterion may be rewritten in the form (Chaboche, 1989):

$$f = J_2(\sigma) - R - \mathrm{k} \tag{2}$$

where k is the initial size of the yield surface and R is the isotropic hardening parameter that can be expressed as a function of the equivalent plastic strain ε_p:

$$R = R(\varepsilon_p) \tag{3}$$

with ε_P defined through

$$d\varepsilon_p = \sqrt{\frac{2}{3} d\varepsilon_p : d\varepsilon_p} \tag{4}$$

and J_2 denotes the von-Mises distance in the deviatoric stress space:

$$J_2(\sigma) = \sqrt{\frac{3}{2}\sigma' : \sigma'} \tag{5}$$

where σ and σ' are the stress and stress deviatoric tensors in the stress space. The flow rule associated with the yield function has the general form (Lemaitre and Chaboche, 1994):

$$\mathrm{d}\varepsilon^P = \mathrm{d}\lambda \frac{\partial f}{\partial \sigma} = \frac{3}{2}\mathrm{d}\lambda \frac{\sigma'}{R + k} \tag{6}$$

where the constant $\mathrm{d}\lambda$ is defined $\mathrm{d}\lambda = \mathrm{d}\varepsilon_P$

The isotropic hardening can be introduced using the evolution of the size of the yield surface as (Chaboche, 1989):

$$\mathrm{d}R = b(Q - R)\mathrm{d}\varepsilon_P \tag{7}$$

where Q and b are two material coefficients. Integrating the above equation with the initial value R = 0 and considering Eq. (2) gives:

$$\sigma^0 = k + Q[1 - \exp(-b.\varepsilon_p)] \tag{8}$$

where σ^0 is the instantaneous yield surface size.

2.2. Kinematic hardening

The classical linear kinematic hardening rule and different nonlinear kinematic hardening models are available for the plastic analysis of structures. The nonlinear kinematic hardening model was first proposed by Armstrong and Frederick (1966). Nonlinearities are given as a recall term in the Prager rule. So that the transformation of yield surface in the stress space is different during loading and unloading. This is done by assuming different hardening modulus in loading and unloading conditions. The yield function for time independent plasticity, using the von-Mises yield criterion, is expressed as (Lemaitre and Chaboche, 1994):

$$f = J_2(\sigma - X) - k \tag{9}$$

where X is the back stress tensor, k the initial size of the yield surface, and J_2 denotes the von-Misses distance in the deviator stress space:

$$J_2(\sigma - X) = [\frac{3}{2}(\sigma' - X') : (\sigma' - X')]^{\frac{1}{2}} \tag{10}$$

Where σ and X are the stress and back stress tensors, and σ' and X' are the stress and back stress deviatoric tensors in the stress space, respectively. The nonlinearities are given as a recall term in the Prager rule:

$$\mathrm{d}X = \frac{2}{3} C \, \mathrm{d}\varepsilon^P - \gamma X \, \mathrm{d}\varepsilon_P \tag{11}$$

Where $\mathrm{d}\varepsilon_P$ is the equivalent plastic strain rate, C and γ are two material dependent coefficients in the Armstrong-Frederick kinematic hardening model, and $\gamma = 0$ stands for the linear kinematic rule.

The normality hypothesis and the consistency condition $\mathrm{d}f = 0$ lead to the expression for the plastic strain rate (Lemaitre and Chaboche, 1994):

$$\mathrm{d}\varepsilon^P = \mathrm{d}\lambda \frac{\partial f}{\partial \sigma} = \frac{H(f)}{h} \left\langle \frac{\partial f}{\partial \sigma} : \mathrm{d}\sigma \right\rangle \frac{\partial f}{\partial \sigma} \tag{12}$$

Where H denotes the Heaviside step function: $H(f) = 0$ if $f < 0$, $H(f) = 1$ if $f \geq 0$ and the symbol $\langle\rangle$ denotes the MacCauley bracket, i.e., $\langle u \rangle = (u + |u|)/2$.

The hardening modulus h becomes:

$$h = C - \frac{3}{2} \gamma X : \frac{\sigma' - X'}{k} \tag{13}$$

In the case of tension –compression, the criterion and the equations of flow and hardening can be expressed in the form (Lemaitre and Chaboche, 1994):

$$f = |\sigma - X| - k = 0 \tag{14}$$

$$\mathrm{d}\varepsilon^p = \frac{1}{h} \left\langle \frac{\sigma - X}{k} \mathrm{d}\sigma \right\rangle \frac{\sigma - X}{k} = \frac{\mathrm{d}\sigma}{h} \tag{15}$$

$$\mathrm{d}X = C\,\mathrm{d}\varepsilon_P - \gamma X\left|\mathrm{d}\varepsilon_P\right| \tag{16}$$

$$h = C - \gamma X\ \mathrm{Sgn}(\sigma - X) \tag{17}$$

The evolution equation of hardening can be integrated analytically to give:

$$X = \nu\frac{C}{\gamma} + (X_0 - \nu\frac{C}{\gamma})\exp[-\nu\gamma(\varepsilon_P - \varepsilon_{P0})] \tag{18}$$

where $\nu = \pm 1$ according to the direction of flow, and ε_{P0} and X_0 are the initial values. For example at the beginning of each plastic flow.

2.3. Nonlinear combined isotropic/kinematic hardening

In the kinematic hardening models, the center of the yield surface moves in the stress space due to the kinematic hardening component. In addition, when the nonlinear isotropic/kinematic hardening model is used, the yield surface range may expand due to the isotropic component. These features allow modeling of inelastic deformation in metals that are subjected to cycles of load or temperature, resulting in significant inelastic deformation and, possibly, low-cycle fatigue failure.

The evolution law of this model consists of two components: a nonlinear kinematic hardening component, which describes the translation of the yield surface in the stress space through the back stress X , and an isotropic hardening component, which describes the change of the equivalent stress defining the size of the yield surface R as a function of plastic deformation.

The kinematic hardening component is defined to be an additive combination of a purely kinematic term (linear Ziegler hardening law) and a relaxation term (the recall term), which introduces the nonlinearity. When temperature and field variable dependencies are omitted, the hardening law is:

$$\mathrm{d}X = C\frac{1}{R}(\sigma - X)\mathrm{d}\varepsilon_P - \gamma X\ \mathrm{d}\varepsilon_P \tag{19}$$

where C and γ are the material parameters that must be calibrated from the cyclic test data. Here, C is the initial kinematic hardening modulus and γ determines the rate at which the kinematic hardening modulus decreases with increasing the plastic deformation. The kinematic hardening law can be separated into a deviatoric part and a hydrostatic part; only the deviatoric part has an effect on the material behavior. When C and γ are zero, the model reduces to an isotropic hardening model. When γ is zero, the linear Ziegler hardening law is recovered.

The isotropic hardening behavior of the model defines the evolution of the yield surface size R as a function of the equivalent plastic strain ε_P. This evolution can be introduced by specifying R as a function of ε_P by using the simple exponential law

$$R = k + Q(1 - e^{-b\varepsilon_P}) \tag{20}$$

where K is the yield stress at zero plastic strain and Q and b are the material parameters. Here, Q is the maximum change in the size of the yield surface and b defines the rate at which the size of the yield surface changes as plastic straining develops. When the equivalent stress defining the size of the yield surface remains constant (R=K), the model reduces to a nonlinear kinematic hardening model.

3. Material and experimental

The experimental arrangements used for testing plain cylinders and other pressurized piping components have been reported in references (Yahiaoui et al., 1992). It is sufficient to give a brief outline of the technique. Cylindrical specimens were machined from carbon steel and stainless steel (304L). Choosing an appropriate material hardening model will be indispensable to proper numerical simulation of the cyclic loading on metallic component. To obtain correct kinematic/isotropic hardening parameters, it is recommended that the hardening model to be calibrated against experimental data in strains close to the strain ranges and loading history expected to occur in the actual application (Zakavi et al). In the current study, the necessary stress–strain data has been collected from tests on small bars (see Fig. 1), remained.

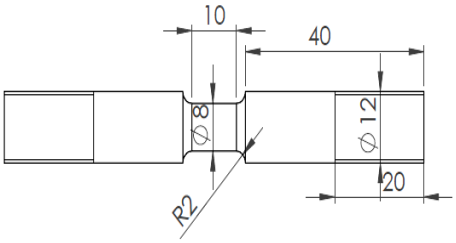

Fig. 1. Shapes and sizes of specimens

The hot-rolled bar of the material was first treated by solution heat treatment at 1050 ^{0}C for 30 minutes and water quench and carbon steel each subjected to several stabilized stress cycles. Different symmetric strain cycles have been considered for each testing bar. The calibration procedure consisted of three bar tests, one of which was subjected to monotonic tension until necking and others were put under symmetric strain-controlled cycles with different strain levels. During these calibration tests, the stress state essentially remained uni-axial. The material parameters for the isotropic hardening exponential law k, Q and b can be derived from monotonic standard tensile test data, where k is the initial size of the yield surface and Q and b are two material coefficients. The material parameters C and γ for the kinematic hardening model have to be

determined by conducting separate tests. Three different approaches are usually used for providing experimental data for evaluating these two parameters:

- Half-cycle test data,
- Single stabilized cycle data.
- Test data obtained from several stabilized cycles.

A typical stress–strain curve for carbon steel and stainless steel is included in Fig. 2. It should be noted that all values of stress given above and in Fig. 2 are engineering stress, mechanical properties of steels is obtained that is shown in Table 1.

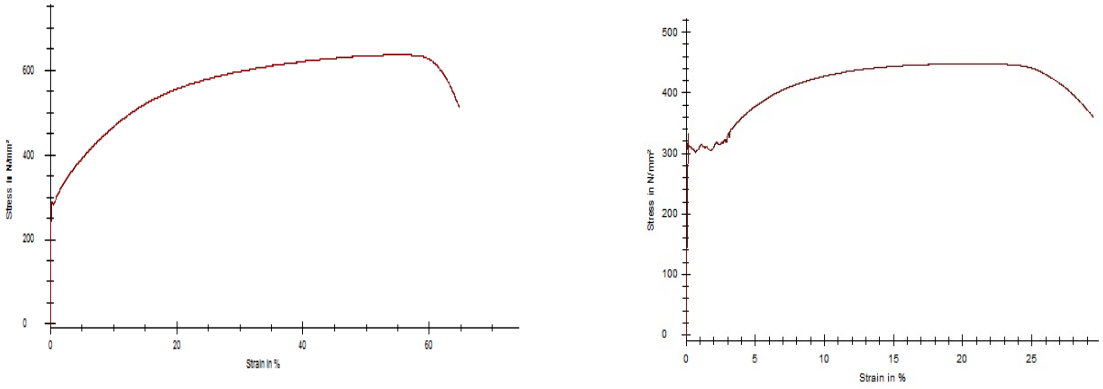

a) b)

Fig. 2**.** Monotonic tensile stress–strain curves at room temperature. a) Stainless steel b) Carbon steel used to manufacture specimens

Table 1

Properties of steel obtained by tensile tests

	Stainless steel	Carbon steel
Young's modulus	195 GPa	212 GPa
(σ_y) Yield stress	292 MPa	324 MPa
Ultimate stress	638MPa	455 MPa
Elongation at failure (%)	64.84%	29.46%

In the current study the latter approach has been used, for which stress–strain data have been obtained from several stabilized cycles on specimens subjected to symmetric strain that are subjected to symmetric strain cycles. By doing the tension-pressure tests with strain control, the model hardening constants can be determined.

Fig.3. INSTRON 8502 servo hydraulic machine.

For this purpose we used of INSTRON 8502 machine (Fig. 3) to obtained stabilized cycles data (see fig 4 to 6). C and γ parameters (Eqs. 11; 19), determine components of kinematic hardening model. The materials used in this work are SS304L stainless steel and carbon steel. Specify the material parameters of the isotropic hardening model of the exponential law K, Q and b directly if they are already calibrated from test data. The material parameters C and γ determine the kinematic hardening component of the model.

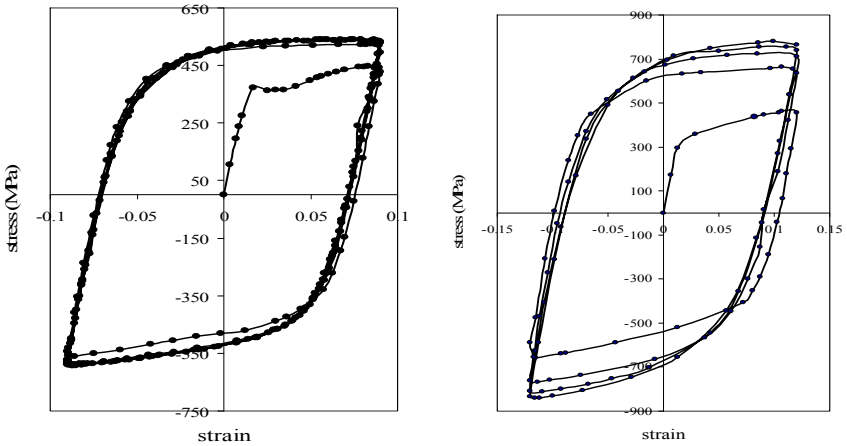

Fig. 4. Hysteresis curve obtained from test for the (a) stainless steel and (b) carbon steel at room temperature

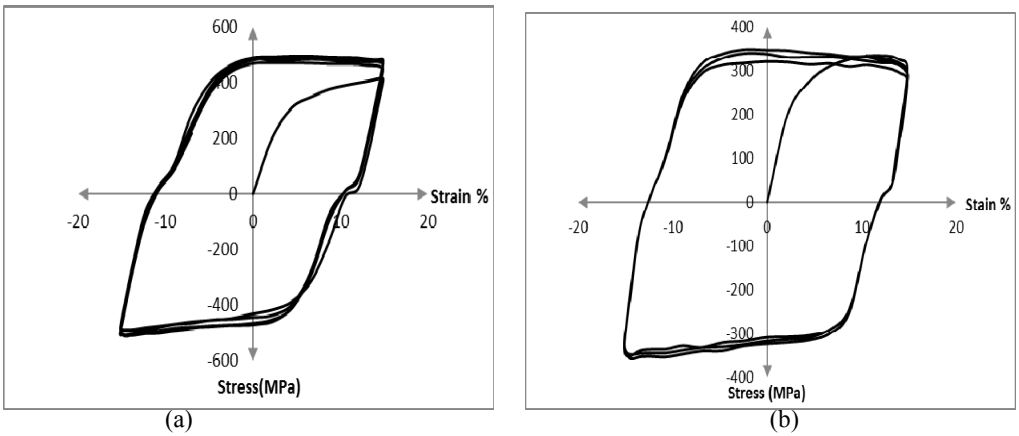

(a) (b)

Fig. 5. Hysteresis curve obtained from test for the (a) stainless steel and (b) carbon steel at 600^0c temperature

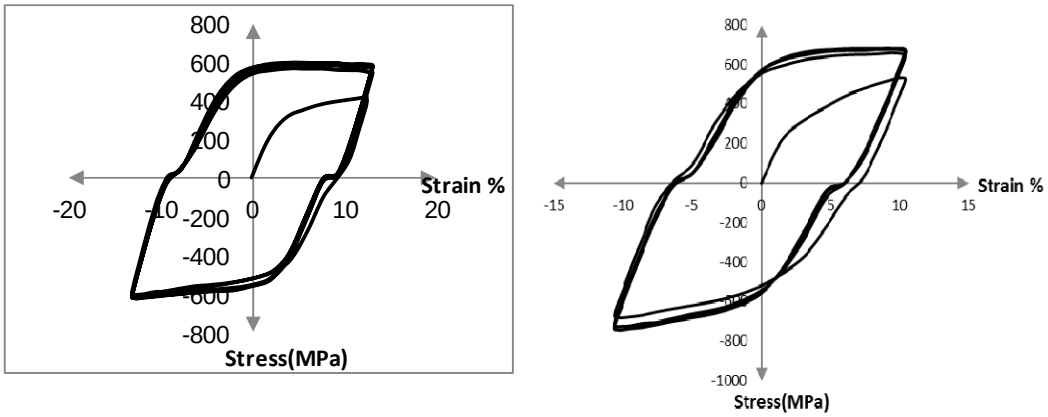

(a) (b)

Fig. 6. Hysteresis curve obtained from test for the (a) stainless steel and (b) carbon steel at 350^0c temperature

The calibration procedure consists of several cylindrical bar tests, one of which subjected to monotonic tension until necking and others were under symmetric strain-controlled experiments with different strains. (Third method). Samples of the stabilized cycles for stainless steel and carbon steel are shown in Figs. 5a and b. During testing, the equivalent plastic strain is:

$$\bar{\varepsilon}_p = \sum_i \left|\Delta\varepsilon_{\mathrm{p(i)}}\right| = \sum_i \left|\Delta\varepsilon_i - \Delta\bar{\sigma}_{\exp} E\right| \tag{21}$$

Where ε_i is the total strain, $\bar{\sigma}_{\exp}$ is the measured stress and E is the elastic modulus.

The method that is used in this paper to specify hardening parameters in Chaboche combined hardening model is using of test data obtained from several stabilized cycles. For this purpose half of the elastic stress domain, k, the stress domain $\Delta\sigma$, and plastic strain range $\Delta\varepsilon_p$, from stabilized cycles for every specimen are obtained. With these results, corresponding ($\frac{\Delta\varepsilon_p}{2}$, $\frac{\Delta\sigma}{2}-k$) data pairs may be plotted, and the kinematic hardening parameters, C and γ, may be calculated by fitting Eq. (22) to the data and selecting parameters minimize the sum of the square of the error between Eq. (22) and the data (Sheldon, 2008).

$$\frac{\Delta\sigma}{2}-k=\frac{C}{\gamma}\tanh(\gamma\frac{\Delta\varepsilon_p}{2}) \tag{22}$$

The results are given for stainless steel and carbon steel in Figs. 7a and b.

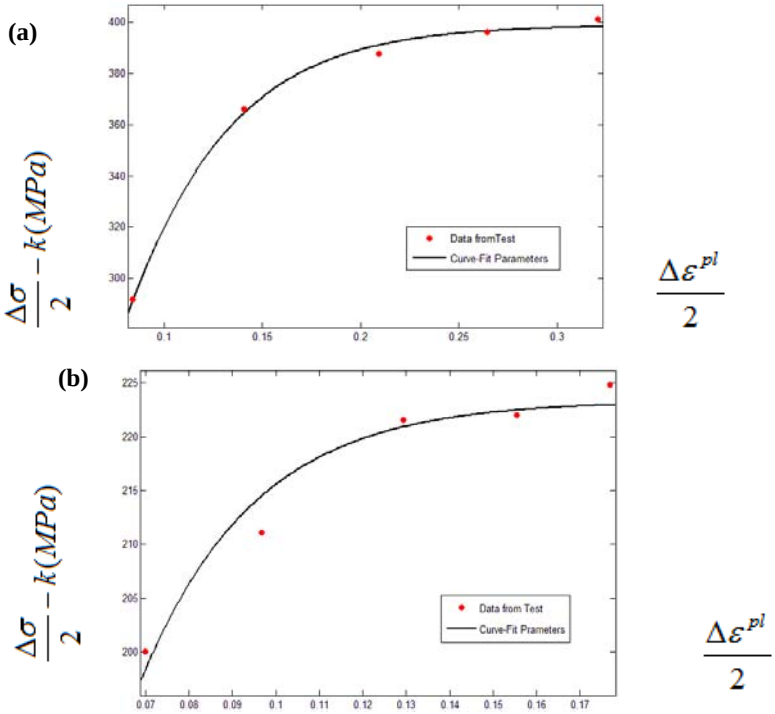

Fig. 7. Curve-fit data for obtain kinematic hardening constants for the (a) stainless steel and (b) carbon steel at room temperature

Using half-cycle test data and using the following equation, the material constants, m and n are determined (Zakavi et al, 2009).

$$\bar{\sigma} = \sigma_y (1 + \frac{\bar{\varepsilon}_p}{m})^n \tag{23}$$

In this equation, $\bar{\sigma}$ is the equivalent stress and σ_y is the initial uniaxial yield stress. Upon fitting Eqs. (18) and (23) to the experimental data, $\bar{\sigma}$ and $\bar{X}$ are known for any equivalent plastic strain, and the isotropic component of the hardening, σ^0, may be defined as a function of equivalent plastic strain by:

$$\sigma^0(\bar{\varepsilon}_p) = \bar{\sigma}(\bar{\varepsilon}_p) - \bar{X}(\bar{\varepsilon}_p) \tag{24}$$

The isotropic material parameters, Q and b, can be determined by fitting Eq. (24) to the results of Eq. (8) and using least-squares nonlinear regression. A typical Curve-fit data for Q and b calibration for stainless steel and carbon steel are shown in Figs. 8a and b. The values of hardening constants for stainless steel and carbon steel are given in Table 2.

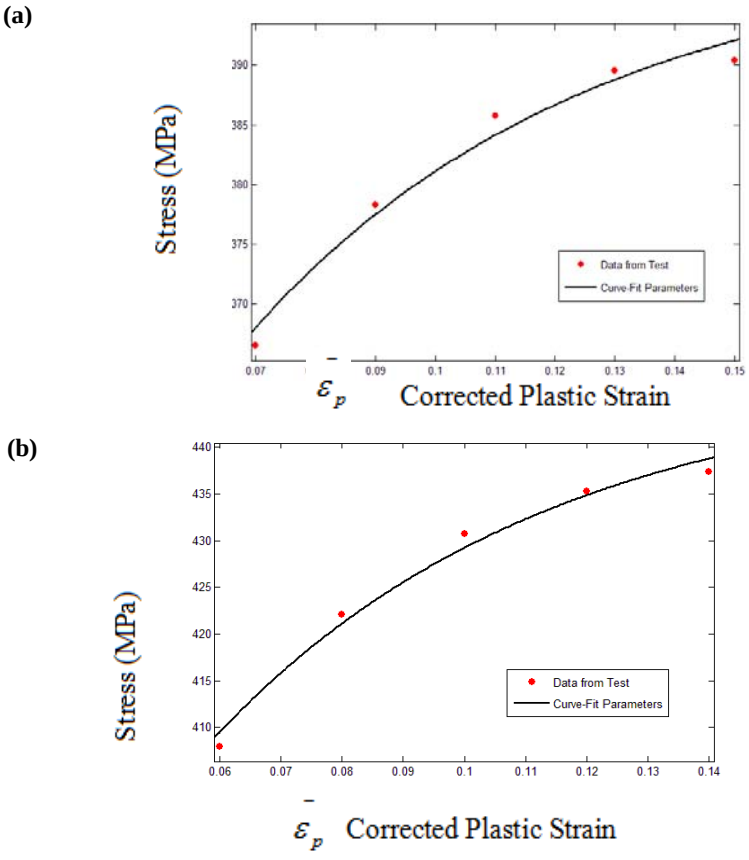

Fig. 8. Curve-fit data for obtain isotropic hardening constants for the (a) stainless steel and (b) carbon steel at room temperature

Table 2

Values of hardening constants for stainless steel and carbon steel

Material	Experiment	$C(MPa)$	γ	$Q(MPa)$	b	T(°c)
Stainless steel	Stabilized cycles	4402.7	11.04	109.6	17.8	20
		1814.58	18.74	365.6	28.78	350
		1260.03	21.26	284.66	32.56	600
Carbon steel	Stabilized cycles	4510.7	20.2	113.7	18.9	20
		3847.48	26.88	494.85	30.09	350
		1628.27	14.19	289.77	55.64	600

4. Conclusions

For using nonlinear isotropic/kinematic (combined) hardening model to predict thermal ratcheting, kinematic hardening parameters C, γ and also isotropic hardening parameters k, b, Q have been obtained from the monotonic and cyclic tests at 350^0c and 600^0c using strain controlled condition experimentally.

R E F E R E N C E S

[1]. *M. Abdel-Karim,* "Numerical integration method for kinematic hardening rules with partial activation of dynamic recovery term*", Int. J. of Plasticity,* **21**:1303-1321, 2005.

[2]. *M. Abdel-Karim, N. Ohno,* "Kinematic hardening model suitable for ratcheting with steady-state", *Int. J. of Plasticity,* **16**:225-240, 2000.

[3]. *P.J.Armstrong, C.O. Frederick,* "A mathematical representation of the multi axial Bauschinger effect", *CEGB* Report RD/B/N 731, Central Electricity Generating Board. The report is reproduced as a paper: 2007. *Materials at High Temperatures*, **24**(1):1-26, 1966.

[4]. *S.Bari, T. Hassan,* "Anatomy of coupled constitutive models for ratcheting simulation", *Int. J. of Plasticity*, **16**:381-409, 2000.

[5]. *S.,Bari, T.Hassan*, "Kinematic hardening rules in uncoupled modeling for multiaxial ratcheting simulation", *Int. J. of Plasticity,* **17**, 2001, pp.885-905.

[6]. *J.Bree,* "Elastic plastic behavior of thin tubes subjected to internal pressure and intermittent high heat fluxes with application to fast nuclear reactor fuel elements", J Strain Anal;**2**(3), pp.226–38, 1967.

[7]. *J.Bree* "Plastic deformation of a closed tube due to interaction of pressure stresses and cyclic thermal stresses", Int Mech Sci.; **31**(11-12), pp.865–92, 1989.

[8]. *J.Cao, W.Lee,, H.S.Cheng, M.Seniw, H-P.Wangc, and* K.Chung, "Experimental and numerical investigation of combined isotropic-kinematic hardening behavior of sheet metals"*, Int. J. of Plasticity*, **(25)**, pp.942–972, 2009.

[9]. *J.L.Chaboche,* "Constitutive equations for cyclic plasticity and cyclic viscoplasticity", *Int. J. of Plasticity***, 5**, pp.247-302, 1989.
[19]. *J.L.Chaboche,* "On some modifications of kinematic hardening to improve the description of ratcheting effects", *Int. J. of Plasticity*, **7**, pp.661-678, 1991.
[20[*J.L.Chaboche,* "Modeling of ratcheting: evaluation of various approaches", *European J. of Mechanics A/Solids*, **13**, pp.501-518, 1994.
[21]. *J.L.Chaboche,* "A review of some plasticity and viscoplasticity constitutive theories", *Int. J. of Plasticity*, **24**, pp.1642-1963, 2008,
[22]. *M.R. Eslami, H.Mahbadi,* "Cyclic loading of thermal stress", *J. of Thermal Stress*, **24**(6):577-603, ISSN: 1521-074X (electronic) 0149-5739 (paper), 2001.
[23]. *Lee, Hyeong-Yeon, J.B. Kim,* "Thermal ratchetting deformation of a 316L stainless steel cylindrical structure under an axial moving temperature distribution". J.Of Pressure Vessels and Piping, Pages 41-48, 2002.
[24]. *J. Lemaitre, J.L Chaboche,* "Mechanics of Solid Materials", Published by Cambridge University Press, ISBN 0521477581, 9780521477581, 584 pages, 1994.
[25]. *N.Ohno, Y.Takahashi, and K.Kuwabara,* "Constitutive modeling of anisothermal cyclic plasticity of 304 stainless steel", ASME J. Eng. Mater. Technol. 111, pp.107–112, 1989.
[26]. *N.Ohno*, "Recent topics in constitutive modeling of cyclic plasticity and viscoplasticity", Appl. Mech., Rev. 43, 1990, pp.283–295, 1989.
[27]. *N.Ohno*, "Constitutive modeling of cyclic plasticity with emphasis on ratchetting", Int. J. Mech. Sci., **40**, pp.251–261,1998.
[28]. *N.Ohno, M.Abdel-Karim,* "Uniaxial ratchetting of 316FR steel at room temperature: II. Constitutive modeling and simulation", ASME J. Eng. Mater. Technol. 122, pp.35–41,2000.
[29]. *W.Prager,* "A new method of analyzing stresses and strains in work-hardening plastic solids", J. Appl. Mechanics, **23**, pp.493-496,1956.
[30]. *H.Tasnim, T.Lakhdar and K.Shree,* "Influence of non-proportional loading on ratcheting responses and simulations by two recent cyclic plasticity models", *Int. J. of Plasticity*, **(24)** , pp.1863–1889, 2008.
[31]. *K.Yahiaoui, D.G. Moffat and D.N.Moreton,* "Techniques for the investigation of the ratchetting behavior of piping components under internal pressure and simulated seismic loadings", *Strain***, 28***(2), pp.53-59, 1992*.
[32]. *M.Zehsaz, S.J.Zakavi, H.Mahbadi and M.R.Eslami,* "Cyclic strain accumulation of plain stainless steel pressurized cylinders subjected to dynamic bending moment", ANSI-JAS, **8**(18) pp.3129-3138, 2008.
[33]. *S.J.Zakavi, M,Zehsaz and MR.Eslami,* "The ratcheting behavior of pressurized plain pipework subjected to cyclic bending moment with the combined hardening model", J Nucl Eng;**240**, pp.726–737, Des 2010.
[34]. *I.Sheldon,* "Chaboche nonlinear kinematic hardeninig model", STI0805, ANSYS Release: 11, 2008.
[35]. *Wada Hiroshi, Ueta Masahiro and Ichimiya Masakazu,* "Proposal of New Estimation Method of Thermal Ratchetting Behavior of Fast BreederReactor Components", Journal of Nuclear Engineering and Design, pp.519-526, 1995.
[36]. *H.Wada, H.Kaguchi, Ueta, M., Ichimiya, M., Kimura, Y.K.Fukuda and I. M.Suzuk*, "Proposal of a New Estimation Method forThethermal Ratcheting of a Cylinder Subjected to Moving Temperature Distribution", Nuclear Engineering and Design,**Vol. 139**, pp. 261–267, 1993.

[37]. *D.R.Miller*,"Thermal Stress Ratchet Mechanism in Pressure Vessel", journal of Basic Engineering, Trans .ASME **81**, pp. 190-196, 1959.

[38]. *UGA, Takeo,* "An Experimental Study on Thermal – Stress Ratchettingof Austenitic Stainless Steel by a Three Bars Specimen", NuclearEngineering and Design, Vol. 26, pp 326-335, 1974.